CHAPTER 1

MULTISCALE SEISMIC TOMOGRAPHY OF MANTLE PLUMES AND SUBDUCTING SLABS

DAPENG ZHAO

Geodynamics Research Center, Ehime University, Matsuyama 790-8577, Japan;
E-mail: zhao@sci.ehime-u.ac.jp

Abstract
Local, regional and global tomographic studies of mantle plumes and subducting slabs are reviewed. Applications of the well-established local and teleseismic tomography methods to subduction zones have resulted in clear images of subducting slabs and magma chambers in the upper mantle wedge beneath active arc volcanoes, indicating that geodynamic systems associated with arc magmatism and back-arc spreading are related to deep processes, such as convective circulation in the mantle wedge and dehydration reactions of the subducting slab. Evidence also shows that arc magma and slab dehydration may also contribute to the generation of various types of earthquakes in subduction zones. Most of the slab materials are stagnant in the mantle transition zone before finally collapsing down to the core-mantle boundary as a result of large gravitational instability from phase transitions. Because most hotspots are located in poorly instrumented continental and oceanic regions, 3-D crust and upper mantle structure is determined for only a few hotspots such as Iceland, Yellowstone and Eifel which are covered by seismic networks. Plume-like low-velocity anomalies are revealed in the upper mantle under those hotspots. Global tomographic studies of deep mantle plumes have just started, and more efforts are needed to image the conduits of the lower-mantle plumes. A thorough understanding of the seismic structure of mantle plumes and subducting slabs will only be achieved by a combination of more effective seismic imaging techniques and dense coverage of global seismic networks, particularly in the oceans.

1 INTRODUCTION

Seismic tomography is a technique for determining the three-dimensional (3-D) structure of the Earth's interior by combining information from a large number of crisscrossing seismic waves triggered by natural or artificial seismic sources (Fig. 1). According to the data used, there are body-wave tomography and surface-wave tomography. According to the scales of the study areas, there are global tomography

D. A. Yuen et al. (eds.), Superplumes, 7–30.

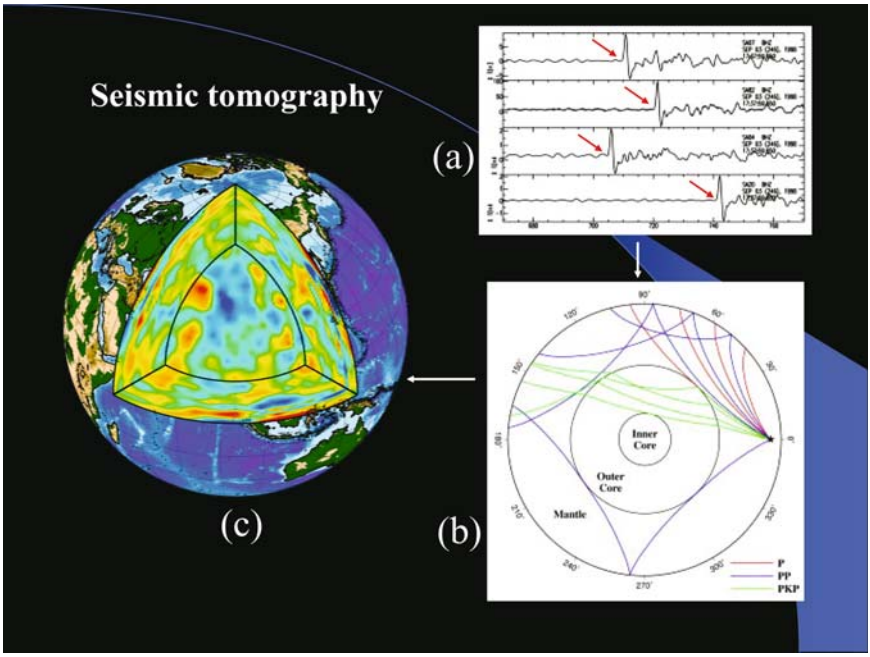

Figure 1. A conceptual diagram of seismic tomography. A large number of arrival times are collected from observed seismograms (a), then a ray tracing technique is used to compute theoretical travel times and ray paths in the Earth's interior (b). Inverting the travel time residuals (differences between the measured and theoretical travel times) results in the three-dimensional distribution of seismic velocity in the Earth (c).

and local/regional tomography. The pioneer studies of the body-wave tomography are Aki and Lee (1976) and Aki et al. (1977) for the local and regional scale, and Dziewonski et al. (1977) and Dziewonski (1984) for the global scale. The surface-wave tomography was initiated by Nakanishi and Anderson (1982), Woodhouse and Dziewonski (1984), and Tanimoto and Anderson (1984). Generally speaking, surface-wave tomography has a lower resolution because of the long wavelength nature of surface waves, and so it is more appropriate for global or large-scale regional studies. By contrast, body-wave tomography can have a much higher spatial resolution because of the short wavelengths of body waves, and it can be applied to multiscale (local, regional and global) studies of the Earth's structure. However, surface-wave tomography is more powerful than body-wave tomography for studying the upper mantle structure under oceanic regions because few stations exist in the oceans. Due to the sparse and uneven coverage of the global seismic networks, global tomographic models still have a low resolution (>500 km), but the models provide information on the deep structure of the Earth. By contrast, local and regional tomographic models for some regions like Japan and California have a much higher

resolution (20–40 km), thanks to the dense seismic networks and much seismicity there, but they are mainly for the crust and/or shallow mantle structures. Because of these advantages and limitations of each of the tomographic approaches, it is necessary to study mantle plumes and subducting slabs by combining useful information from the multiscale tomographic models.

Subducting lithospheric slabs and ascending mantle plumes could be the two complementary features of mantle convection (Nataf, 2000). Subducting slabs represent the main downwellings of mantle convection, while the main upwellings of mantle convection are concentrated in hot columnar features, i.e., plumes. Not all kinds of thermal convection must assume this structural form for the upwellings, but a long series of theoretical investigations has by now established the consensus that ascending flow in the mantle is organized in plume-like structures (Cserepes and Yuen, 2000). The mantle plume hypothesis was proposed forty years ago by Wilson (1963) and Morgan (1971) to explain hotspot volcanoes such as Hawaii and Iceland. A mantle plume is a buoyant mass of material in the mantle that rises because of its buoyancy. On reaching the base of the lithosphere, the plume heads may reach diameters of 500–3000 km, while plume tails are typically 100–500 km in diameter. Hotspots are the surface manifestation of mantle plumes and are focused zones of melting. They are characterized by high heat flow, active volcanism, variable topographic highs depending on plume depth, and hotspot tracks with the age of magmatism and deformation increasing with distance from a hotspot (Condie, 2001). Hotspots and mantle plumes hold the key to several crucial issues of mantle dynamics, and geoscientists are now fully aware of their geodynamical importance (Maruyama, 1994; Condie, 2001). Maruyama (1994) proposed a plume tectonics theory, emphasizing the dominant role of plumes and particularly superplumes in the dynamic evolution of the Earth. In the multidisciplinary effort engaged in understanding hotspots and plumes better, the first task assigned to seismologists is the detection of mantle plumes (Nataf, 2000).

The principles and early developments of seismic tomography were summarized and reviewed by Thurber and Aki (1987), Iyer (1989) and Zhao (2001a). Studies of global and surface-wave tomography were covered by Montagner (1994) and Romanowicz (2003). Shallow and deep structures of subduction zones are reviewed by Zhao (2001b) and Fukao et al. (2001), respectively. Nataf (2000) reviewed the seismic studies of mantle plumes in the twentieth century. In this chapter I review the recent advances in the multiscale tomographic studies of subducting slabs and mantle plumes.

2 LOCAL AND REGIONAL TOMOGRAPHY

Seismologists have mainly used two methods to conduct local and regional tomographic imagings. One is local earthquake tomography (LET) which uses arrival times from local earthquakes recorded by a network of seismic stations; both earthquakes and seismic stations are located in the study area (e.g., Aki and Lee, 1976;

Thurber, 1983; Zhao et al., 1992). The other is teleseismic tomography which uses relative travel time residuals from teleseismic events (distant earthquakes or nuclear explosions) recorded by a seismic network (e.g., Aki et al., 1977). In the latter case, seismic stations are located within the study area, while seismic events are located far from the study area, usually 30–100 degrees (1 degree = 111.2 km) from the edge of the study region. The two methods have inherent advantages and drawbacks. LET can determine the shallow structure of an area to a depth above which earthquakes occur or diving rays (like Pn waves) propagate, but cannot determine the deeper structure. In contrast, teleseismic tomography can determine the deep structure of an area (the maximum modeling depth is about 1.5 times the aperture of the seismic network used), but usually cannot determine the shallow structure since teleseismic rays basically travel in a vertical direction and do not crisscross well near the surface. To resolve this problem, local earthquake arrival times and teleseismic data can be used jointly (e.g., Zhao et al., 1994, 1997). This joint inversion approach preserves the advantages of the two separate approaches and overcomes their drawbacks. Moreover, the horizontally propagating local rays and vertically traveling teleseismic rays crisscross well in the shallow portion of the model, which improve the resolution there.

2.1 Crust and upper mantle structure of subduction zones

Subduction zones have long been recognized as key elements in plate tectonics. Subduction and arc magmatism are fundamental processes in the evolution of the Earth. They play critical roles in the present day differentiation of the Earth's material and are believed to be the major sites of the generation of the continental crust. Subduction is also significant in the water and carbon cycles. So far numerous seismological studies have been made in order to understand the subduction processes, and the 3-D crust and upper mantle structure of most subduction zones has been investigated by using LET or teleseismic tomography methods (see reviews by Zhao, 2001b and Stern, 2002). According to these previous studies, seismological features of subduction zones can be summarized as follows.

All kinds of earthquakes occur in the crust and upper mantle under subduction zones. Shallow earthquakes mainly occur in the upper crust down to about 20 km depth. In the lower crust and uppermost mantle low-frequency microearthquakes ($M < 2.0$) occur only in localized small areas right beneath active volcanoes, which are considered to be associated with the activity of arc magma chambers (Ukawa and Obara, 1993; Hasegawa and Yamamoto, 1994). Recently it has been found that low-frequency microearthquakes occur widely in the forearc regions of Southwest Japan and Cascadia subduction zones, which are considered to be associated with the dehydration process of subducting slabs (Obara, 2002; Rogers and Dragert, 2003). Intermediate-depth and deep-focus earthquakes occur only in the subducting slabs which are colder than the surrounding mantle by a few hundred degrees, and they form a clear Wadati-Benioff deep seismic zone. In some regions the Wadati-Benioff zone may show a two-layered structure (double seismic zone) (Hasegawa et al.,

1978). A majority of seismicity in subduction zones, particularly the large and great earthquakes, occur in the dipping main thrust zone from the oceanic trench down to 40–60 km depth, which reflect the seismic and mechanical coupling between the subducting oceanic plate and the overlying continental plate (e.g., Kanamori, 1971; Stern, 2002).

The subducting oceanic slabs are imaged clearly by seismic tomography as high-velocity anomalies with P and S wave velocities 4–8% faster than the surrounding mantle (Zhao et al., 1992, 1994) (Fig. 2). The subducting slabs also exhibit lower attenuation (high-Q) than the surrounding mantle (Tsumura et al., 2000; Stachnik et al., 2004). The thickness of the slabs seems to depend on the slab age; it is 30–35 km under Kyushu and Southwest Japan (Zhao et al., 2000; Zhao, 2001b), 50 km under Alaska (Zhao et al., 1995), and 90–100 km under NE Japan and Tonga (Zhao et al., 1994, 1997) (Fig. 2).

Structural heterogeneity is expected to exist within the subducting slabs, and it is actually revealed by detailed analysis of seismic waves passing through the slabs. A thin low-velocity (low-V) layer is detected on the top of the slab, which is interpreted to be the subducting oceanic crust (Matsuzawa et al., 1986). Abers (2005) investigated the structure of the low-V layer under seven circum-Pacific arcs and detected a wave guide extending to greater than 150 km depth with a low-V channel 2–8 km thick and with velocity reductions as large as 14% compared with the surrounding mantle,

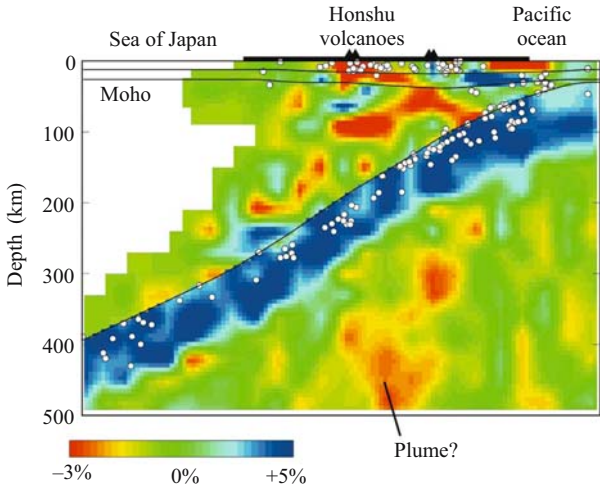

Figure 2. East–west vertical cross section of P-wave velocity structure along a profile passing through central Japan. Red and blue colors denote slow and fast velocities, respectively. The velocity perturbation scale is shown at the bottom. White dots denote earthquakes that occurred within a 40-km width from the profile. The thick bar and solid triangles denote the land area and active arc volcanoes, respectively. The three curved lines show the Conrad and the Moho discontinuities and the upper boundary of the subducting Pacific plate (Zhao, 2004).

although there is substantial variability with depth. It is found that intermediate-depth earthquakes in the lower plane of the double seismic zone under NE Japan occur in relatively higher-velocity areas within the slab (Zhao et al., 1992). The existence of a metastable olivine wedge within the subducting slab was proposed to explain the occurrence of the intermediate-depth and deep-focus earthquakes (Green and Burnley, 1989; Kirby, 1991). However, it is still debatable whether such a metastable olivine wedge really exists and, and even if it does exist, whether it can be detected (Koper et al., 1998).

Prominent low-V and low-Q (high attenuation) zones are imaged by seismic tomography in the upper mantle wedge above the subducting slab in all the subduction zones investigated so far, which represent the arc magma chambers associated with the slab dehydration and convective circulation process in the mantle wedge (Zhao et al., 1992, 1997; Zhao, 2001b) (Fig. 2). Shear wave splitting analyses have shown that strong seismic anisotropy exists in the mantle wedge (Nakajima and Hasegawa, 2004). Tamura et al. (2002) found along-arc variation of the low-V zones in the mantle wedge under NE Japan, suggesting that mantle melting and the production of magmas may be controlled by locally developed hot regions within the mantle wedge that have the form of inclined, 50 km wide fingers. The hot fingers in the mantle wedge under NE Japan are also modelled by numerical simulations (Honda and Saito, 2003).

So far 3-D seismic structure of the crust and upper mantle has been determined under the land areas of many subduction zones. The structure of the forearc region under oceanic areas, however, is less well known because earthquakes under the oceans are not located accurately due to the lack of seismic stations. Umino et al. (1995) detected sP depth phase from seismograms of earthquakes under the Pacific Ocean recorded by land seismic stations in NE Japan and used the sP phase to relocate the sub-oceanic events accurately, since the sP phase is very sensitive to the focal depth. This approach is used to relocate many earthquakes under the NE Japan forearc beneath the Pacific Ocean; and then P and S wave data from earthquakes beneath both the land and Pacific Ocean are combined to determine 3-D P and S velocity structures under the entire NE Japan arc from the Japan trench to the Japan Sea coast (Zhao et al., 2002; Mishra et al., 2003; Wang and Zhao, 2005). Their inversion results revealed strong lateral heterogeneities on the upper boundary of the Pacific slab under the forearc region, which show a good correlation with the spatial distribution of large interplate earthquakes. Widespread slow anomalies are visible in the forearc mantle above the subducting Pacific slab, which may reflect the serpentinization of the forearc mantle associated with the dehydration process of the subducting slab. Fluids from the slab dehydration and lateral heterogeneity on the slab boundary can certainly affect the nucleation of large interplate earthquakes in the forearc region (Zhao et al., 2002). These studies have the important implications that detailed tomographic images can be obtained outside a seismic network if earthquakes occur there. Applying the new approach to other subduction zones would greatly advance our understanding of the structure and dynamics of the forearc regions.

2.2 Upper mantle structure of hotspots and mantle plumes

Hotspots have an irregular but nonrandom distribution over the Earth's surface. They are preferentially located near the divergent plate boundaries (mid-ocean ridges), and are preferentially excluded from regions near the convergent plate boundaries, in particular, subduction zones (Stefanick and Jurdy, 1984; Richards et al., 1988; Weinstein and Olson, 1989). There is little agreement on the total number of hotspots. Several hotspot lists have been published and the number of hotspots included on these lists ranges from about 20 to more than 100 (Morgan, 1972; Wilson, 1973; Crough and Jurdy, 1980; Vogt, 1981). On recent lists the number of hotspots converges to 44 (Steinberger, 2000) to 47 (Richards et al., 1988). The origin of these hotspots is generally attributed to mantle plumes (Wilson, 1963; Morgan, 1971), but some intraplate volcanism may be explained by plate tectonic processes in the upper mantle and the mantle transition zone (Anderson, 2000; Foulger, 2003).

Compared with subduction zones, the seismic structure of the crust and mantle is less well known for most of the hotspots and mantle plumes. The main reason for this seems to be that most of the hotspots are located in the oceanic regions and the African continent where few seismic stations exist, posing problems for seismic imaging. The upper mantle structure under only a few hotspots has been studied by seismic imaging.

The best studied hotspot is Iceland, partly because the island is large enough to install permanent and portable seismic networks for imaging its 3-D upper mantle structure (Tryggvason et al., 1983; Wolfe et al., 1997; Foulger et al., 2000; Allen et al., 2002; Hung et al., 2004). These studies show that a cylindrically shaped low-V zone extends from the shallow upper mantle to 400 km depth beneath central Iceland. The low-V anomalies in the depth range of 250–400 km are elongated in the N-S direction, which is interpreted as an indication of the upper mantle origin of the upwelling beneath the hotspot (Foulger et al., 2000). Hung et al. (2004) used finite frequency tomography to image the Iceland plume. Their results show a columnar low-V zone having a lateral dimension of ~250–300 km extends to 670 km depth, deeper than that resolved by the ray-based studies. Receiver function analyses using P to S conversions from upper mantle discontinuities show that the mantle transition zone beneath central and southern Iceland is thinned, consistent with the hypothesis that the Iceland plume originates from deeper than 700 km (Shen et al., 2002).

Hawaii is a prototypal hotspot and has the largest buoyancy flux of all active plumes (Sleep, 1990). It is one of the most thoroughly studied hotspots in the world by various geophysical, geochemical and petrological methods, yet there remain fundamental geodynamic questions regarding the nature of mantle flow and plume-lithosphere interaction in the region. Several seismic studies in the Hawaiian region have characterized aspects of the local mantle structure. Tomographic inversions of teleseismic data have yielded images of low-V anomalies down to 350 km depth, which have been taken to indicate the presence of melt migrating upward to the active volcanoes (Ellsworth and Koyanagi, 1977; Tilmann et al., 2001; Wolfe et al., 2002). The inversions did not resolve a cylindral low-V plume in the upper mantle beneath the

islands of Hawaii, but resolution tests indicate that this outcome could be the result of the sparse and nearly linear distribution of seismic stations combined with the incomplete azimuthal coverage of the earthquake sources (Wolfe et al., 2002). Measurements of Rayleigh wave dispersion have been carried out to assess the presence of a hot asthenosphere emanating from the plume and the degree of downstream lithospheric erosion (Woods and Okal, 1996; Priestley and Tilmann, 1999; Laske et al., 1999). Mantle discontinuities beneath the islands have been mapped using receiver functions (Li et al., 2000). While these results have been promising, the limited distribution of seismic stations in these experiments has left open the full nature of the mantle seismic structure beneath the Hawaiian hotspot. A determination of the detailed 3-D structure of the upper mantle beneath the Hawaiian hotspot will require a simultaneous deployment of both ocean-bottom and land seismometers (Wolfe et al., 2002).

Yellowstone is the best known continental hotspot. As it propagated across eastern Idaho to its current location in NW Wyoming, it left behind a swath of magmatically altered crust, the eastern Snake River Plain, which lies along the axis of a SW broadening wake-like swell. This behavior is consistent with mantle melt release at a focused site that is stationary in a hotspot reference frame, and with the hot and buoyant residuum flattening against the base of the lithosphere as it is dragged to the SW by the motion of the North American plate. Several teleseismic tomography studies have been made for this region (Evans, 1982; Saltzer and Humphreys, 1997; Schutt and Humphreys, 2004; Yuan and Dueker, 2005). A 100-km diameter upper mantle plume is imaged that extends from the Yellowstone volcanic caldera to 500 km depth. A monotonic decrease in the velocity perturbation of the plume from −3.2% at 100 km to −0.9% at 450 km is consistent with a uniform thermal anomaly of 180°C (Yuan and Dueker, 2005).

Ritter et al. (2001) and Keyser et al. (2002) showed P and S wave images of the upper mantle below the Quaternary Eifel volcanic fields, Germany, determined by teleseismic tomography. They measured the data at a dedicated seismic network of more than 200 stations. Their results show a columnar low-V anomaly in the upper mantle. The 100 km wide structure extends to at least 400 km depth and is equivalent to ∼150–200 K excess temperature. This clear evidence for a plume below a region of comparatively minor volcanism suggests that deep mantle plumes could be more numerous than commonly assumed (Malamud and Turcotte, 1999), which may often be associated with small volcanic fields or may have no volcanic surface expression at all. Global tomographic studies show a wide plume-like structure in the lower mantle below Central Europe, but no clear connection through the transition zone to the shallow mantle (Goes et al., 1999; Zhao, 2001c).

Pilidou et al. (2004) showed a S-wave velocity and azimuthal anisotropy model for the upper mantle beneath the North Atlantic and surrounding region derived from analyses of over 3000 fundamental and higher mode Rayleigh waveforms. Their model has a horizontal resolution of a few hundred kilometers extending to 400 km depth. Low-V anomalies in the vicinity of the Eifel hotspot extend to about 400 km depth. Strong slow anomalies exist in the North Atlantic upper mantle beneath the

Iceland and Azores hotspots. Both anomalies are, above 200 km depth, 5–7% low and are elongated along the Mid-Atlantic ridge. The fast propagation direction of S waves in the Atlantic south of Iceland correlates well with the E-W ridge-spreading direction at all depths and changes to a direction close to N-S in the vicinity of Iceland.

2.3 Intraplate volcanism in Northeast Asia

Several active intraplate volcanoes, e.g., Wudalianchi and Changbai, exist in NE Asia (Figs. 3 and 4). The Wudalianchi volcano erupted in AD 1719 and 1721. The Changbai volcano erupted in AD 1050, 1120, 1193 and 1410. The origin of these volcanoes is still unclear. Some researchers considered them to be hotspots (e.g., Turcotte and Schubert, 1982), while others invoked the asthenospheric injection to explain them (Tatsumi et al., 1990). Recently 3-D seismic images of the mantle down

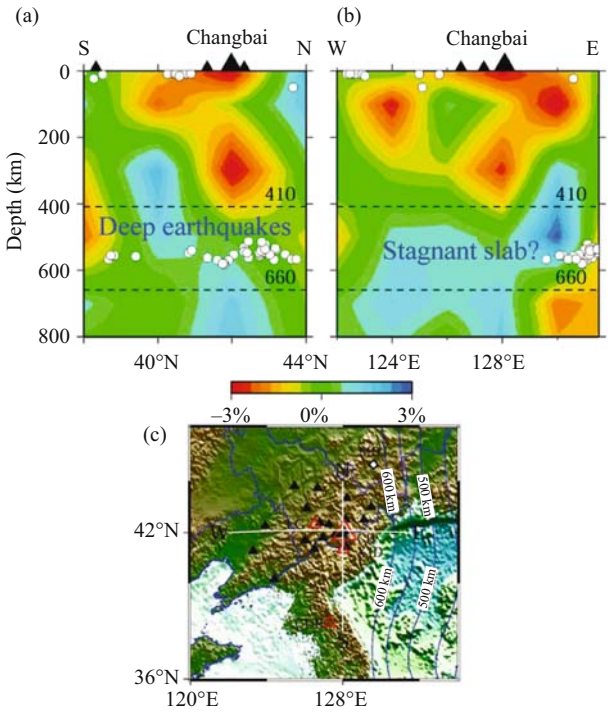

Figure 3. North–south (a) and east–west (b) vertical cross sections of P-wave velocity images under the Changbai intraplate volcano in NE Asia (Zhao et al., 2004). Red and blue colors denote slow and fast velocities, respectively. The velocity perturbation scale is shown below the cross sections. Black triangles in (a) and (b) denote the intraplate volcanoes. White dots denote earthquakes that occurred within 100 km of the profiles. The two dashed lines denote the 410 and 660 km discontinuities. (c) Locations of the cross sections in (a) and (b). Black and red triangles denote seismic stations and volcanoes, respectively. The contour lines show the depths of the Wadati-Benioff deep seismic zone.

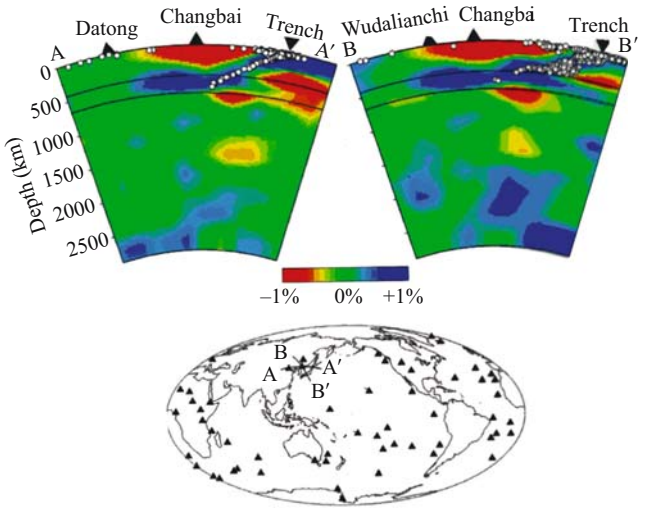

Figure 4. Vertical cross sections of P-wave velocity images determined by a global tomographic inversion (Zhao, 2004). Locations of the cross sections are shown in the insert map. Red and blue colors denote slow and fast velocities, respectively. The velocity perturbation scale is shown below the cross sections. Black triangles denote volcanoes. The reversed triangles show the location of the Japan Trench. White dots denote earthquakes that occurred within 150 km of the profiles. The two solid lines denote the 410 and 660 km discontinuities.

to 800 km depth are determined beneath the Changbai volcano by applying teleseismic tomography to relative travel time residuals recorded by a portable seismic network (Zhao et al., 2004; Lei and Zhao, 2005) (Fig. 3). The results show a columnar low-V anomaly extending to 400 km depth under the Changbai volcano. High-velocity anomalies are visible in the mantle transition zone, and deep earthquakes occur at depths of 500–600 km under the region, suggesting that the subducting Pacific slab is stagnant in the transition zone, as imaged clearly also by global tomography (Zhao, 2004) (Fig. 4).

The tomographic images under NE Asia are quite similar to those under the Fiji-Tonga region where the back-arc volcanoes in Fiji and the Lau spreading center are located above very slow anomalies in the mantle wedge right above the subducting Tonga slab (Zhao et al., 1997). These results suggest that the active volcanoes in NE Asia are not hotspots like Hawaii but a sort of back-arc volcanoes which are closely related to the subduction process of the Pacific slab. Low-V anomalies in the back-arc region are generally associated with the back-arc magmatism and volcanism caused by the deep dehydration process of the subducting slab and the convective circulation process of the mantle wedge (Zhao et al., 1994, 1997; Zhao, 2001b). These processes lead to the large-scale upwelling of the asthenospheric materials under NE Asia and cause intraplate volcanism and continental rift systems in the region. The extensional rift systems and faults widely existing in NE Asia may be the surface manifestation

of the deep dynamic processes (Tatsumi et al., 1990). Tatsumi et al. (1990) first proposed the asthenospheric injection to explain the formation of the Wudalianchi and Changbai volcanoes, but they did not consider the stagnant Pacific slab under the region because such a slab structure was unknown at that time. Zhao et al. (2004) emphasized the role of the stagnant Pacific slab in the formation of the intraplate volcanism in NE Asia.

2.4 The Baikal rift zone

The Baikal rift zone is composed of a branched chain of Late Cenozoic half-grabens extending over a distance of about 1500 km in Siberia with significant seismic and volcanic activities. It is situated at the boundary of the Siberian platform (craton) to the northwest and the Mongolian fold belt to the southeast. Lake Baikal occupies only about a third of the rift zone. It is the deepest lake (1620 m) in the world and contains 20% of the world's fresh water. The Baikal rift is probably the most debated of all rifts in terms of its origin. Most Russian scientists support the active rift hypothesis that theorizes an anomalous upper mantle that formed beneath the continental lithosphere and led to the development of the rift. The passive hypothesis suggests the rift began as a result of the collision of India with Asia. These disagreements are mainly caused by the fact that the deep structure of the Baikal rift zone has not been understood well, although many researchers have studied the crust and upper mantle structure under this region using various geophysical methods including seismic tomography.

Zhao et al. (2006) carefully collected a large number of high-quality arrival time data from original seismograms of teleseismic events recorded by a portable seismic network; they used a modified tomographic inversion method (Zhao, 2001c) to determine the P-wave velocity images under the Baikal rift zone. Their results show a prominent low-velocity anomaly extending down to 600 km depth under the Baikal rift zone and high-velocity anomalies in the lithosphere under the Siberian craton. The low-velocity anomalies are interpreted as a mantle upwelling (plume) which has played an important role in the initiation and evolution of the Baikal rift zone. The rift formation may also be controlled by other factors such as older (prerift) linear lithosphere structures favorably positioned relative to the upwelling and favorable orientation of the far-field forces caused by the India-Asia collision.

3 GLOBAL SEISMIC TOMOGRAPHY

During the last two decades, many global tomographic studies have been made to determine the whole mantle 3-D structure (Dziewonski, 1984; Inoue et al., 1990; Zhang and Tanimoto, 1993; Su et al., 1994; Vasco et al., 1995; Grand et al., 1997; van der Hilst et al., 1997; Bijwaard et al., 1998; Boschi and Dziewonski, 1999; Ritsema et al., 1999; Zhao, 2001c, 2004). Forward waveform modeling has complemented tomographic studies, providing details of structural features as well as smaller-scale patterns of heterogeneity (see reviews by Lay et al., 1998 and Garnero, 2000). These studies have greatly improved our understanding of the structure and dynamics of

the Earth's deep interior. In past studies of travel-time tomographic inversions for the mantle structure, a few researchers have carefully measured their own arrival time data (Woodward and Master, 1991; Su et al., 1994; Grand et al., 1997); many others have used the large International Seismological Center (ISC) data set. Although the ISC data have been critiqued because of uncertainties in travel time picking methods, a careful reprocessing of the data (Engdahl et al., 1998) has resulted in global images of mantle structure from ISC P times that look remarkably similar to those from non-ISC S times (Grand et al., 1997).

So far most of the global tomographic studies have concentrated on the imaging of deep subducting slabs, and much has been found out about the cold parts of the mantle convection. The upwelling plumes, the hot portion of the mantle convection, however, have been focused only by a few recent global tomographic studies (Bijwaard and Spakman, 1999; Zhao, 2001c, 2004; Montelli et al., 2004).

3.1 Deep structure of subducting slabs

Many seismological studies in the last two decades have addressed the issue of the fate of subducting oceanic slabs, in particular, the behavior of slabs around the 670 km discontinuity. Earlier researchers (e.g., Creager and Jordan, 1984, 1986) thought that slabs simply plunge directly through the 670 km discontinuity. Later, tomographic images showed complex behavior of the subducted slabs (e.g., Zhou, 1996; Grand et al., 1997; van der Hilst et al., 1997; Bijwaard et al., 1998; Fukao et al., 2001; Zhao, 2001c, 2004). Their results do not support a simple slab penetration, but show a strong resistance when the slab encounters the 670 km discontinuity. The slab bends horizontally, and accumulates there for a long time (ca. 100–140 m.y.), and then finally collapses to fall down as blobs onto the core mantle boundary (CMB) as a result of very large gravitational instability from phase transitions (Machetel and Weber, 1991; Honda et al., 1993; Cadek et al., 1994; Maruyama, 1994) (Fig. 4). But there are still different opinions on the depth range of the slab stagnancy. Fukao et al. (2001) suggested that slabs are stagnant in the so-called Bullen transition zone at depths of 400–1000 km. In contrast, the tomographic images of Boschi and Dziewonski (1999) and Zhao (2001c, 2004) show that strong and wide high-velocity anomalies exist in the mantle transition zone (410–670 km) under the subduction regions. In the top portion of the lower mantle, the circum-Pacific high-velocity zone becomes less clear or disappears. Zhao (2004) conducted several synthetic tests and confirmed it to be a reliable feature.

Receiver functions and waveform modeling analyses show complicated features in the depth range of 660–780 km at the tip of the stagnant slab as well as reflectors/scatters in the lower mantle under the subduction region in the western Pacific (Niu and Kawakatsu, 1996; Tajima et al., 1998; Kaneshima and Helffrich, 2003; Ai et al., 2003). This phenomenon is considered to be caused by the pieces of slab blobs collapsing down to the lower mantle.

Many tomographic models show the images of the old Farallon slab in the lower mantle under North America, and it is generally agreed that the Farallon slab has

sunk deeply through the lower mantle reaching the CMB (e.g., Grand et al., 1997; Bijwaard et al., 1998; Fukao et al., 2001; Zhao, 2004). Other deeply sinking slabs are the presumed Indian (Tethys) slab under Himalaya and the Bay of Bengal as well as Mesozoic slabs under Siberia (Van der Voo et al., 1999a,b). These remanent slabs are not connected to the surface plates or to the presently subducting slabs and appear to sink independently from the latter. The presence of these deeply sinking slabs implies that the pre-Eocene subduction occurred in much the same way as in the present day to accumulate slab bodies in the transition zone and that the consequent unstable down flow occurred extensively through the transition region in the Eocene epoch to detach many of the surface plates from the subducted slabs at depths and hence caused the reorganization of the global plate motion (Fukao et al., 2001).

An unexpected feature in Figure 4 is that prominent slow anomalies appear beneath the subducting Pacific slab and extend down to the lower mantle. This feature was also imaged by Fukao et al. (2001). To understand this feature better, Zhao (2004) conducted a high-resolution tomographic inversion using arrival times of local and teleseismic rays recorded by the dense seismic networks on the Japan Islands. The tomographic image obtained has a spatial resolution of 25–35 km for the crust and mantle wedge and 40–50 km for the subducting slab and the mantle under the slab down to a depth of 500 km (Fig. 2). The subducting Pacific slab and arc-magma related slow anomalies in the mantle wedge are imaged clearly. Prominent slow anomalies are visible in the depth range of 260–500 km under the subducting Pacific slab. The sub-slab slow anomalies have a lateral extent of 70–160 km. Reconstruction tests and resolution analyses confirmed that they are a reliable feature. It is unclear what the sub-slab slow anomalies represent. There are two possibilities: one is that they represent a hot upwelling portion of a local-scale convection associated with the subduction of the Pacific slab; the other is that they show a small mantle plume rising from the lower mantle (see also Fig. 4). Malamud and Turcotte (1999) suggested that more than 5000 plumes exist in the mantle and the large number of seamounts represents the surface evidence for small plumes. If this conjecture is correct, it is not surprising that small plumes appear under the subducting slab, as detected by the tomographic imagings (Figs. 2 and 4).

3.2 Deep mantle plumes

Although most of the global tomographic studies in the last two decades have showed that seismic velocity is slower in the lower mantle under South-Central Pacific and Africa where most hotspots are located, little effort was made to exploit the tomographic models to address the deep structure and origin of mantle plumes. Bijwaard and Spakman (1999) were perhaps the first attempt to address this issue. Their global P-wave tomographic model revealed a continuous low-V anomaly of 500–600 km wide in the lower mantle under the Iceland hotspot, which was interpreted as the Iceland plume originating from the CMB. Ritsema et al. (1999) developed a global S-wave tomographic model derived from surface-wave and body-wave data. Their model shows that vertically continuous low-V anomalies in the upper mantle are

present beneath Afar, Bowie, Easter, Hawaii, Iceland, Louisville, McDonald and Samoa hotspots but not beneath the other 29 hotspots in the list of Sleep (1990). Low-V zones are also visible in the lower mantle under some of the hotspots, but the authors were not certain about those features due to the limited resolution of their model (see also Ritsema and Allen, 2003).

Zhao (2001c) developed a global P-wave tomography model particularly for detecting mantle plumes. He inverted about one million data of P, pP, PP and PcP waves selected from the reprocessed ISC data set (Engdahl et al., 1998). His model shows two superplumes under South Pacific and Africa, which have lateral extents of thousands of kilometers and exist in the whole mantle (Fig. 5). Continuous whole-mantle plumes are also detected under Hawaii, Iceland and Kerguelen hotspots (Fig. 5). The Hawaiian plume is not part of the Pacific superplume, but it is possible that there are some heat or material interchanges between them in the mid-mantle depth (Zhao, 2004; Lei and Zhao, 2006). Some small-scaled plumes are also found, which originate from the transition zone or mid-mantle depths. An important result of Zhao (2001c, 2004) is that slow anomalies under hotspots usually do not show a straight pillar shape, but exhibit winding images (Fig. 5), which suggests that plumes are not fixed in the mantle but can be deflected due to the influence of mantle flow, as was

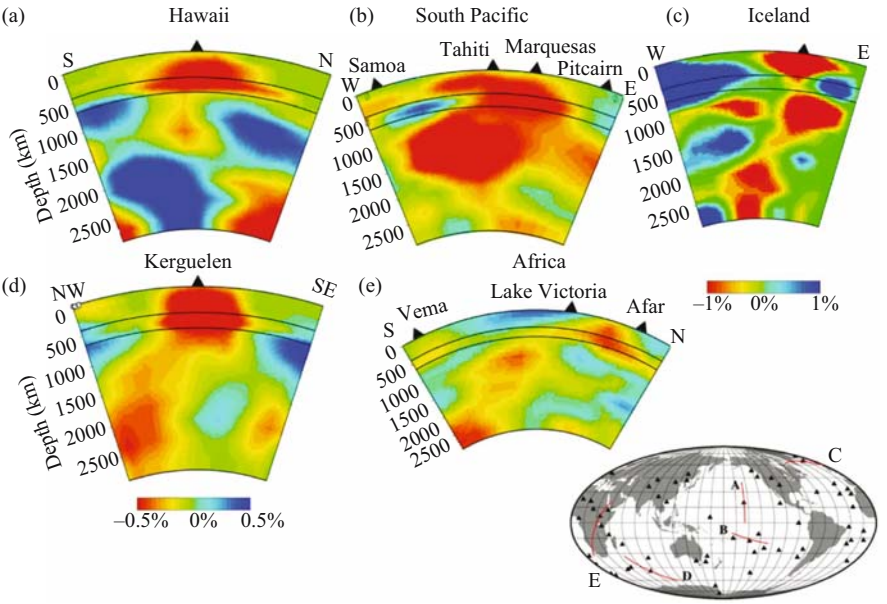

Figure 5. Vertical cross sections of P-wave velocity images under Hawaii (a), South Pacific (b), Iceland (c), Kerguelen (d), and Africa (e) derived from the global tomographic model of Zhao (2004). Locations of the cross sections are shown in the insert map. Red and blue colors denote slow and fast velocities, respectively. The velocity perturbation scale is shown below (c) and (d). Black triangles denote the hotspot volcanoes. The two solid lines in each of the cross sections denote the 410 and 660 km discontinuities.

pointed out earlier by numerical simulation studies (e.g., Griffiths and Richards, 1989; Loper, 1991; Steinberger, 2000). Other seismic imagings (Bijwaard and Spakman, 1999; Shen et al., 2002) and paleomagnetic studies (Tarduno and Cottrell, 1997) also suggested the deflection of plumes. As a consequence of the deflection of mantle plumes, hotspots would not be fixed in the long geological history but could wander on the Earth's surface, though their relative moving velocities are much smaller than those of the lithospheric plates (Molnar and Stock, 1987; Griffiths and Richards, 1989; Tarduno and Cottrell, 1997; Steinberger, 2000).

Montelli et al. (2004) determined a global P-wave tomographic model using a finite-frequency modeling and irregular model parameterizations. Their model shows a collection of plumes in the mantle. Deep plumes are present beneath Ascension, Azores, Canary, Cape Verde, Cook Island, Easter, Kerguelen, Samoa and Tahiti. Plumes rising from the base of the mantle but not yet reaching the surface are located in the Coral Sea, east of Solomon and south of Java. Plumes beneath Eifel, Etna and Seychelles remain mostly confined to the upper mantle. Several plume images extend only down to the mid-mantle. For these plumes a deep origin cannot be simply ruled out because resolution tests show that they could have a very thin, not resolvable, tail. Also, none of the imaged plumes exhibits the typical mushroom-shaped structure. Their model also shows that the plumes are wide, with radii as large as 300–400 km. However, the effectiveness of the finite-frequency tomography and the tomographic model of Montelli et al. (2004) have been questioned and criticized recently (de Hoop and van der Hilst, 2005; van der Hilst and de Hoop, 2005).

In addition to global tomography, several waveform modeling studies also suggested the lower mantle or CMB origin of the Hawaiian plume (Ji and Nataf, 1998; Russell et al., 1999) and the Iceland plume (Helmberger et al., 1998; Shen et al., 2002). Foulger et al. (2000) proposed that the Iceland plume extends down to the mantle transition zone and no deeper. However, their tomographic images were based on the data recorded by a local seismic network and so have no resolution below the transition zone.

It is still a debated issue what causes the hotspots and whether plumes exist. Instead of the plume hypothesis, some mechanisms associate hotspot formation to propagating cracks, abandoned ridges, leaky transforms or other damaged regions of the lithosphere that is under extention and above a partially molten upper mantle (McDougall, 1971; Turcotte and Oxburgh, 1973; Anderson, 2000; Fougler, 2003). Convection due to thermal gradients at the margins of cratonic lithosphere and passive infilling processes along the mid-ocean ridge produce 3-D instabilities that may be indistinguishable from plume upwellings (King and Anderson, 1995; King and Ritsema, 2000; Korenaga and Jordan, 2002).

3.3 Heterogeneity in the lowermost mantle

The lowermost 200 km of the mantle (known as the D″ region) has long been characterized by seismologists as distinctive in its properties from the overlying deep mantle. The D″ and CMB regions have undoubtedly played a significant role

in both the core and mantle dynamic systems throughout the 4.50-Gyr evolution of the Earth (Lay et al., 1998). Numerous studies have revealed the presence of anomalous features in the D″ region, such as intermittent stratification, shear-wave anisotropy and ultra-low-velocity layer (see reviews by Lay et al., 1998 and Garnero, 2000). These seismic observations and their spatial systematics raise many questions about primary processes in the CMB region and possible importance of the CMB layer for dynamic processes throughout the planet, including an intimate relationship to subducted slabs and mantle plumes as well as surface structures, which define challenging research frontiers for experimental and computational geophysics. But the precise role of the CMB region remains a topic of vigorous research and debate requiring improved resolution of the structure and processes operating there.

The D″ and CMB regions are thought to be the graveyard of subducted slabs and the birth place of mantle plumes. It has been proposed that the large slow regions in the mantle beneath the central Pacific and Africa, observed in all tomographic models, are related to superplumes generated by thermal boundary layer instabilities at the CMB (Stacey and Loper, 1983; Sleep, 1990; Thompson and Tackley, 1998). It was also found that some parts of the D″ regions under south-central Pacific and Africa exhibit ultralow velocities, which are interpreted as partial melts (Williams and Garnero, 1996). Some chemical heterogeneity, possibly involving core material (iron), may be present as well (Knittle and Jeanloz, 1991). It is dynamically possible for the heavier iron to be pulled upward by strong enough thermal buoyant forces, as shown in numerical simulations (Hansen and Yuen, 1988; Yuen et al., 1993; Cadek et al., 1994).

Prominent high-velocity patches are also visible in the lowermost mantle. Waveform modeling studies show that some areas have a contrast of 7–8% with respect to adjacent "hot" mantle, which cannot be explained by thermal effects alone (Breger and Romanowicz, 1998). A portion of ancient slab lying at the CMB is not likely to be responsible for this velocity contrast because reconstructions of ancient subduction zones do not predict the presence of a remnant lithosphere in D″ under the south-central Pacific (Lithgow-Bertelloni and Richards, 1998), and such a fossil slab might not produce a sufficient velocity contrast (Wysession et al., 1998). The fast and localized anomaly could represent a high-velocity product of the decomposition of perovskite at temperatures and pressures corresponding to the lowermost mantle (Stixrude, 1998) or of core-mantle reactions (Knittle and Jeanloz, 1991; Stixrude, 1998); and it may be related to the selective entrainment of chemically distinctive material into the thermal plume (Kellogg and King, 1993). Because significant shear wave splitting has been observed for waves traveling through the central Pacific region (Vinnik et al., 1998), the large velocity contrast could also be related to anisotropy. The blocks of fast material on the CMB could be responsible for the intermittent reflections observed at the top of D″ (Garnero, 2000).

Recently a post-perovskite transition in $MgSiO_3$ was found by in situ X-ray diffraction in a diamond anvil cell at ~2500 K and 125 GPa (Murakami et al., 2004). This condition is similar to that expected in the D″ layer. This post-perovskite structure

was also identified by first principles calculations (Tsuchiya et al., 2004). This phase transition is important for understanding the state of the deep lower mantle, particularly that of the D″ layer, e.g., its wide topography and strong anisotropy.

4 DISCUSSION AND CONCLUSIONS

The distribution of both earthquakes and seismic stations on Earth is nonuniform. Earthquakes occur mainly in plate boundary regions; intermediate-depth and deep-focus earthquakes occur only in subduction zones. Seismic stations are installed mainly in a few developed countries on the land areas. In the broad oceanic regions and the African and South American continents, there are few permanent stations; though portable stations were deployed there for short periods of time. This nonuniform nature of the distribution of the seismic sources and stations requires a multiscale approach to seismic imaging. Regions that are covered densely by stations and/or seismicity can be imaged with a high resolution by using teleseismic and local tomography, while poorly instrumented regions can only be imaged roughly by global or large-scale regional tomography. This situation will last for quite a long time. However, a recent study shows that high-resolution local tomography can be obtained without a dense seismic network if reflected and converted waves can be detected from seismograms and used in the tomographic inversion (Zhao et al., 2005).

Compared with other tectonic units on Earth, subduction zones have been well studied by seismological methods. The 3-D seismic structure of the crust and upper mantle under the continental margins and the land areas of island arcs is determined for most of the subduction zones, which revealed the high-velocity subducting slabs and low-velocity anomalies in the mantle wedge under the active arc volcanoes. The formation of arc magmatism and volcanism has been well understood in the last two decades, thanks to the advances in seismic imaging in addition to the petrological and geochemical studies.

There is, however, much to be done for the further understanding of the structure and dynamics of subduction zones. First, little is known on the forearc region of most subduction zones. Determination of the detailed structure of the forearc regions is important for understanding the initial stage of subduction and the seismic and mechanical coupling between the subducting oceanic plate and the overlying continental plate. Most of the large and great earthquakes in the world occur in the forearc regions of subduction zones. Clarification of the generating mechanism of the damaging interplate earthquakes also requires a detailed study of the forearc regions. Second, the back-arc regions need further studies, which are important for understanding the mechanism of back-arc spreading, deep slab dehydration, depth extent of the mantle wedge magma, as well as the relationship between the arc magmatism and the intraplate volcanism in the continental region behind the marginal seas (e.g., the active volcanoes in NE Asia). Third, the detailed structure of the subducting slab should be investigated, which is important for resolving the puzzle of the double seismic zone, the presence or absence of the metastable olivine wedge, and the mechanism of deep-focus earthquakes. Fourth, the structure of the

lower slab boundary and the mantle under the slab is poorly known. Is the lower boundary of the slab a sharp seismic discontinuity as its upper boundary? If not, how thick is the transitional zone around the lower slab boundary? Is the mantle under the slab homogeneous or heterogeneous? If heterogeneity exists there, what is the cause? These questions should be addressed in future studies of subduction zones.

The plume hypothesis is very attractive in explaining the hotspot magmatism and it is now widely recognized. However, direct evidence for actual plumes is weak, and many questions remain unanswered. Do plumes actually exist? What do they look like? How wide are they? How hot are they? Do they really rise from the CMB? All of them? Are they tilted on their way up? Are there different kinds of plumes? (Nataf, 2000). To answer these questions, seismic imaging will play a critical role. So far detailed 3-D crust and upper mantle structure is determined for only a few hotspots such as Iceland, Yellowstone and Eifel. Such information is scarce for most of the hotspots, even the best known one, Hawaii. Since the local and teleseismic tomography methods have been well established and proved to be quite effective, the main remaining work for studying the upper mantle structure of hotspots is the instrumentation. Portable seismic networks should be deployed in every continental hotspot area. For imaging the oceanic hotspots and plumes, ocean bottom seismic networks are necessary, though they are much more expensive and difficult to deploy than the instrumentation on the land.

Global seismic tomography is the most effective tool to determine the deep structure of subducting slabs and mantle plumes. So far most global tomographic studies have been conducted for determining the long-wavelength structures of the mantle and for imaging the slabs, those for detecting plumes have just started. Because most hotspots are located far from the existing seismic stations and earthquake sources, special efforts are needed to collect useful data and to devise tomographic inversions for imaging mantle plumes. A large number of multiple reflected waves from the surface (or ocean floor), such as PP, PPP, SS and SSS waves, should be collected, which, together with surface wave data, can help to image the upper mantle plumes under the oceanic regions. Multiple reflected waves from the CMB (e.g., PcP, PcP2, ScS, ScS2) and diffracted waves at the CMB (Pdiff, Sdiff) should be collected for imaging the plumes in the lower mantle. These later phase data can be collected multitudinously with the modern waveform processing technologies.

Continuous efforts are also needed to improve the theoretical aspects of seismic imaging. The development of an improved theoretical framework, coupled with more powerful computers, has opened the way to new tomographic methods and the possibility of exploiting more fully the richness of broadband seismograms (Romanowicz, 2003). It is clear that the full understanding of the seismic structure of mantle plumes and subducting slabs will only be achieved by a combination of more effective seismic imaging techniques and dense coverage of global seismic networks, particularly in the oceans. The challenge is great, but with ingenuity and cooperation we can anticipate exciting new advances in seismic imaging and the understanding of the Earth's structure and dynamics in the next one to two decades.

ACKNOWLEDGEMENTS

This work was partially supported by Grant-in-aid for Scientific Research (B-11440134 and A-17204037) from the Ministry of Education and Science, Japan, and a special COE grant from Ehime University. The author is grateful to S. Maruyama, D. Yuen, C. Matyska and S. Omori for thoughtful discussion and review comments.

REFERENCES

Abers, G. (2005) Seismic low-velocity layer at the top of subducting slabs: Observations, predictions, and systematics. *Phys. Earth Planet. Inter.*, 149, 7–29.

Ai, Y., T. Zheng, W. Xu, Y. He, and D. Dong (2003) A complex 660 km discontinuity beneath northeast China. *Earth Planet. Sci. Lett.*, 212, 63–71.

Aki, K., and W. Lee (1976) Determination of three-dimensional velocity anomalies under a seismic array using first P arrival times from local earthquakes, 1. A homogeneous initial model. *J. Geophys. Res.*, 81, 4381–4399.

Aki, K., A. Christoffersson, and E. Husebye (1977) Determination of the three-dimensional seismic structure of the lithosphere. *J. Geophys. Res.*, 82, 277–296.

Allen, R., G. Nolet, W. Morgan et al. (2002) Imaging the mantle beneath Iceland using integrated seismological techniques. *J. Geophys. Res.*, 107(B12), JB000595.

Anderson, D. (2000) The thermal state of the upper mantle: No role for mantle plumes. *Geophys. Res. Lett.*, 27, 3623–3626.

Bijwaard, H., and W. Spakman (1999) Tomographic evidence for a narrow whole mantle plume below Iceland. *Earth Planet. Sci. Lett.*, 166, 121–126.

Bijwaard, H., W. Spakman, and E. Engdahl (1998) Closing the gap between regional and global travel time tomography. *J. Geophys. Res.*, 103, 30055–30078.

Boschi, L., and A. Dziewonski (1999) High- and low-resolution images of the Earth's mantle: Implications of different approaches to tomographic modeling. *J. Geophys. Res.*, 104, 25567–25594.

Breger, L., and B. Romanowicz (1998) Three-dimensional structure at the base of the mantle beneath the central Pacific. *Science*, 282, 718–720.

Cadek, O., D.A. Yuen, V. Steinbach, A. Chopelas, and C. Matyska (1994) Lower mantle thermal structure deduced from seismic tomography, mineral physics and numerical modeling. *Earth Planet. Sci. Lett.*, 121, 385–402.

Condie, K. (2001). Mantle Plumes and Their Record in Earth History, Cambridge University Press, Cambridge, UK, 306pp.

Creager, K., and T. Jordan (1984) Slab penetration into the lower mantle. *J. Geophys. Res.*, 89, 3031–3049.

Creager, K., and T. Jordan (1986) Slab penetration into the lower mantle beneath the Mariana and other island arcs of the Northwest Pacific. *J. Geophys. Res.*, 91, 3573–3589.

Crough, S., and D. Jurdy (1980) Subducted lithosphere, hotspots, and the geoid. *Earth Planet. Sci. Lett.*, 48, 15–22.

Cserepes, L., and D. Yuen (2000) On the possibility of a second kind of mantle plume. *Earth Planet. Sci. Lett.*, 183, 61–71.

de Hoop, M., and R. van der Hilst (2005) On sensitivity kernels for wave equation transmission tomography. *Geophys. J. Int.*, 160, 621–633.

Dziewonski, A. (1984) Mapping the lower mantle: Determination of lateral heterogeneity in P velocity up to degree and order 6. *J. Geophys. Res.*, 89, 5929–5952.

Dziewonski, A., B. Hager, and R. O'Connell (1977) Large-scale heterogeneities in the lower mantle. *J. Geophys. Res.*, 82, 239–255.

Ellsworth, W., and R. Koyanagi (1977) Three-dimensional crust and mantle structure of Kilauea volcano, Hawaii. *J. Geophys. Res.*, 82, 5379–5394.

Engdahl, E., R. van der Hilst, and R. Buland (1998) Global teleseismic earthquake relocation with improved travel times and procedures for depth determination. *Bull. Seismol. Soc. Am.*, 88, 722–743.

Evans, J. (1982) Compressional wave velocity structure of the upper 350 km under the eastern Snake River Plain near Rexburg, Idaho. *J. Geophys. Res.*, 87, 2654–2670.

Foulger, G. (2003) Plumes, or plate tectonic processes? *Astron. Geophys.*, 43, 6.19–6.23.

Foulger, G., M. Pritchard, B. Julian, and J. Evans (2000) The seismic anomaly beneath Iceland extends down to the mantle transition zone and no deeper. *Geophys. J. Int.*, 142, F1–F5.

Fukao, Y., S. Widiyantoro, and M. Obayashi (2001) Stagnant slabs in the upper and lower mantle transition region. *Rev. Geophys.*, 39, 291–323.

Garnero, E. (2000) Heterogeneity of the lowermost mantle. *Annu. Rev. Earth Planet. Sci*. 28, 509–537.

Goes, S., W. Spakman, and H. Bijwaard (1999) A lower mantle source for Central European volcanism. *Science*, 286, 1928–1931.

Grand, S., R. van der Hilst, and S. Widiyantoro (1997) Global seismic tomography: A snapshot of convection in the Earth. *GSA Today*, 7, 1–7.

Green, H., and P. Burnley (1989) A new self-organizing mechanism for deep-focus earthquakes. *Nature*, 341, 733–737.

Griffiths, R., and M. Richards (1989) The adjustment of mantle plumes to changes in plate motion. *Geophys. Res. Lett.*, 16, 437–440.

Hansen, U., and D. Yuen (1988) Numerical simulation of thermal chemical instabilities at the core-mantle boundary. *Nature*, 334, 237–240.

Hasegawa, A., and A. Yamamoto (1994) Deep, low-frequency microearthquakes in or around seismic low-velocity zones beneath active volcanoes in northeastern Japan. *Tectonophysics*, 233, 233–252.

Hasegawa, A., N. Umino, and A. Takagi (1978) Double-planed deep seismic zone and upper-mantle structure in the northeastern Japan arc. *Geophys. J. R. Astron. Soc.*, 54, 281–296.

Helmberger, D., L. Wen, and X. Ding (1998) Seismic evidence that the source of the Iceland hotspot lies at the core-mantle boundary. *Nature*, 396, 251–258.

Honda, S., and M. Saito (2003) Small-scale convection under the back-arc occurring in the low viscosity wedge. *Earth Planet. Sci. Lett.*, 216, 703–715.

Honda, S., D.A. Yuen, S. Balachandar, and D. Reuteler (1993) Three-dimensional instabilities of mantle convection with multiple phase transitions. *Science*, 259, 1308–1311.

Hung, S., Y. Shen, and L. Chiao (2004) Imaging seismic velocity structure beneath the Iceland hotspot: A finite frequency approach. *J. Geophys. Res.*, 109, B08305.

Inoue, H., Y. Fukao, K. Tanabe, and Y. Ogata (1990) Whole mantle P wave travel time tomography. *Phys. Earth Planet. Inter.*, 59, 294–328.

Iyer, H. (1989) Seismic tomography. In James, D. (ed.) The Encyclopedia of Solid Earth Geophysics, Van Nostrand Reinhold, New York, pp. 1131–1151.

Ji, Y., and H. Nataf (1998) Detection of mantle plumes in the lower mantle by diffraction tomography: Hawaii. *Earth Planet. Sci. Lett.*, 159, 99–115.

Kanamori, H. (1971) Great earthquakes at island arcs and the lithosphere. *Tectonophysics*, 12, 187–198.

Kaneshima, S., and G. Helffrich (2003) Subparallel dipping heterogeneities in the mid-lower mantle. *J. Geophys. Res.*, 108(B5), JB001596.

Kellogg, L., and S. King (1993) Effect of mantle plumes on the growth of D″ by reaction between the core and mantle. *Geophys. Res. Lett.*, 20, 379–392.

Keyser, M., J. Ritter, and M. Jordan (2002) 3D shear-wave velocity structure of the Eifel plume, Germany. *Earth Planet. Sci. Lett.*, 203, 59–82.

King, S., and D. Anderson (1995) An alternate mechanism of flood basalt volcanism. *Earth Planet. Sci. Lett.*, 136, 269–279.

King, S., and J. Ritsema (2000) African hot spot volcanism: Small-scale convection in the upper mantle beneath cratons. *Science*, 290, 1137–1140.

Kirby, S. (1991) Mantle phase changes and deep-earthquake faulting in subducting lithosphere. *Science*, 252, 216–224.

Knittle, E., and R. Jeanloz (1991) Earth's core-mantle boundary: Results of experiments at high pressure and temperatures. *Science*, 251, 1438–1443.

Koper, K., D. Wiens, L. Dorman, J. Hildebrand, and S. Webb (1998) Modeling the Tonga slab: Can travel time data resolve a metastable olivine wedge? *J. Geophys. Res.*, 103, 30079–30100.

Korenaga, J., and T. Jordan (2002) Effects of vertical boundaries on infinite Prandtl number thermal convection. *Geophys. J. Int.*, 147, 639–659.

Laske, G., J. Morgan, and J. Orcutt (1999) First results from the Hawaiian SWELL pilot experiment. *Geophys. Res. Lett.*, 26, 3397–3400.

Lay, T., Q. Williams, and E. Garnero (1998) The core-mantle boundary layer and deep Earth dynamics. *Nature*, 392, 461–468.

Lei, J., and D. Zhao (2005) P-wave tomography and origin of the Changbai intraplate volcano in Northeast Asia. *Tectonophysics*, 397, 281–295.

Lei, J., and D. Zhao (2006) A new insight into the Hawaiian plume. *Earth Planet. Sci. Lett.*, 241, 438–453.

Li, X., R. Kind, K. Priestley, S. Sobolev, and F. Tilmann (2000) Mapping the Hawaiian plume conduit with converted seismic waves. *Nature*, 405, 938–941.

Lithgow-Bertelloni, C., and M. Richards (1998) The dynamics of Cenozoic and Mesozoic plate motions. *Rev. Geophys.*, 36, 27–78.

Loper, D. (1991) Mantle plumes. *Tectonophysics*, 187, 373–384.

Machetel, P., and P. Weber (1991) Intermittent layered convection in a model mantle with an endothermal phase change at 670 km. *Nature*, 350, 55–57.

Malamud, B., and D. Turcotte (1999) How many plumes are there? *Earth Planet. Sci. Lett.*, 174, 113–124.

Maruyama, S. (1994) Plume tectonics. *J. Geol. Soc. Jpn.*, 100, 24–49.

Matsuzawa, T., N. Umino, A. Hasegawa, and A. Takagi (1986) Upper mantle velocity structure estimated from PS-converted wave beneath the north–eastern Japan arc. *Geophys. J. R. Astron. Soc.*, 86, 767–787.

McDougall, L. (1971) Volcanic island chains and sea floor spreading. *Nature*, 231, 141–144.

Mishra, O., D. Zhao, N. Umino, and A. Hasegawa (2003) Tomography of northeast Japan forearc and its implications for interplate seismic coupling. *Geophys. Res. Lett.*, 30(16), GL017736.

Molnar, P., and J. Stock (1987) Relative motions of hotspots in the Pacific, Atlantic, and Indian oceans since late Cretaceous time. *Nature*, 327, 587–591.

Montagner, J. (1994) Can seismology tell us anything about convection in the mantle? *Rev. Geophys.*, 32, 115–138.

Montelli, R., G. Nolet, G. Master, F. Dahlen, E. Engdahl, and H. Hung (2004) Finite-frequency tomography reveals a variety of plumes in the mantle. *Science*, 303, 338–343.

Morgan, W. (1971) Convection plumes in the lower mantle. *Nature*, 230, 42–43.

Morgan, W. (1972) Deep motions and deep mantle convection. *Geol. Soc. Am. Mem.*, 132, 7–22.

Murakami, M., K. Hirose, K. Kawamura, N. Sata, and Y. Ohishi (2004) Post-perovskite phase transition in MgSiO3. *Science*, 304, 855–858.

Nakajima, J., and A. Hasegawa (2004) Shear-wave polarization anisotropy and subduction-induced flow in the mantle wedge of northeastern Japan. *Earth Planet. Sci. Lett.*, 225, 365–377.

Nakanishi, I., and D. Anderson (1982) World-wide distribution of group velocity of mantle Rayleigh waves as determined by spherical harmonic inversion. *Bull. Seismo. Soc. Am.*, 72, 1185–1194.

Nataf, H. (2000) Seismic imaging of mantle plumes. *Annu. Rev. Earth Planet. Sci.*, 28, 391–417.

Niu, F., and H. Kawakatsu (1996) Complex structure of mantle discontinuities at the tip of the subducting slab beneath northeast China. *J. Phys. Earth*, 44, 701–711.

Obara, K. (2002) Nonvolcanic deep tremor associated with subduction in southwest Japan. *Science*, 296, 1679–1681.

Pilidou, S., K. Priestley, O. Gudmundsson, and E. Debayle (2004) Upper mantle S-wave speed heterogeneity and anisotropy beneath the North Atlantic from regional surface wave tomography: The Iceland and Azores plumes. *Geophys. J. Int.*, 159, 1057–1076.

Priestley, K., and F. Tilmann (1999) Shear-wave structure of the lithosphere above the Hawaiian hotspot from two-station Rayleigh wave phase velocity measurements. *Geophys. Res. Lett.*, 26, 1493–1496.

Richards, M., B. Hager, and N. Sleep (1988) Dynamically supported geoid highs over hotspots: Observation and theory. *J. Geophys. Res.*, 93, 7690–7708.

Ritsema, J., and R. Allen (2003) The elusive mantle plume. *Earth Planet. Sci. Lett.*, 207, 1–12.

Ritsema, J., H. Jan der Heijst, and J. Woodhouse (1999) Complex shear wave velocity structure imaged beneath Africa and Iceland. *Science*, 286, 1925–1928.

Ritter, J., M. Jordan, U. Christensen, and U. Achauer (2001) A mantle plume below the Eifel volcanic field, Germany. *Earth Planet. Sci. Lett.*, 186, 7–14.

Rogers, G., and H. Dragert (2003) Episodic tremor and slip on the Cascadia subduction zone: The chatter of silent slip. *Science*, 300, 1942–1943.

Romanowicz, B. (2003) Global mantle tomography: Progress status in the past 10 years. *Ann. Rev. Earth Planet. Sci.*, 31, 303–328.

Russell, S., T. Lay, and E. Garnero (1999) Small scale lateral shear velocity and anisotropy heterogeneity near the core-mantle boundary beneath the central Pacific imaged using broadband ScS waves. *J. Geophys. Res.*, 104, 13183–13199.

Saltzer, R., and E. Humphreys (1997) Upper mantle P wave velocity structure of the eastern Snake River Plain and its relationship to geodynamic models of the region. *J. Geophys. Res.*, 102, 11829–11842.

Schutt, D., and E. Humphreys (2004) P and S wave velocity and Vp/Vs in the wake of the Yellowstone hot spot. *J. Geophys. Res.*, 109, B01305.

Shen, Y., S. Solomon, I. Bjarnason, and G. Nolet (2002) Seismic evidence for a tilted mantle plume and north–south mantle flow beneath Iceland. *Earth Planet. Sci. Lett.*, 197, 261–272.

Sleep, N. (1990) Hotspots and mantle plumes: Some phenomenology. *J. Geophys. Res.*, 95, 6715–6736.

Stachnik, J., G. Abers, and D. Christensen (2004) Seismic attenuation and mantle wedge temperatures in the Alaska subduction zone. *J. Geophys. Res.*, 109(B10), B10304.

Stacey, F., and D. Loper (1983) The thermal boundary layer interpretation of D″ and its role as a plume source. *Phys. Earth Planet. Inter.*, 33, 45–50.

Stefanick, M., and D. Jurdy (1984) The distribution of hot spots. *J. Geophys. Res.*, 89, 9919–9925.

Steinberger, B. (2000) Plumes in a convecting mantle: Models and observations for individual hotspots. *J. Geophys. Res.*, 105, 11127–11152.

Stern, R. (2002) Subduction zones. *Rev. Geophys.*, 40(4), RG000108.

Stixrude, L. (1998) Elastic constants and anisotropy of MgSiO3 perovskite, periclase, and SiO2 at high pressure. In Gurnis, M., B. Buffett, K. Knittle, M. Wysession (eds.) The Core-Mantle Boundary, AGU, pp. 83–96.

Su, W., R. Woodward, and A. Dziewonski (1994) Degree 12 model of shear velocity heterogeneity in the mantle. *J. Geophys. Res.*, 99, 6945–6980.

Tajima, F., Y. Fukao, M. Obayashi, and T. Sakurai (1998) Evaluation of slab images in the northwestern Pacific. *Earth Planets Space*, 50, 953–964.

Tamura, Y., Y. Tatsumi, D. Zhao, Y. Kido, and H. Shukuno (2002) Hot fingers in the mantle wedge: new insight into magma genesis in subduction zones. *Earth Planet. Sci. Lett.*, 197, 105–116.

Tanimoto, T., and D. Anderson (1984) Mapping convection in the mantle. *Geophys. Res. Lett.*, 11, 287–290.

Tarduno, J., and R. Cottrell (1997) Paleomagnetic evidence for motion of the Hawaiian hotspot during formation of the Emperor seamounts. *Earth Planet. Sci. Lett.*, 153, 171–180.

Tatsumi, Y., S. Maruyama, and S. Nohda (1990) Mechanism of backarc opening in the Japan Sea: Role of asthenospheric injection. *Tectonophysics*, 181, 299–306.

Thompson, P., and P. Tackley (1998) Generation of mega-plumes from the core-mantle boundary in a compressible mantle with temperature-dependent viscosity. *Geophys. Res. Lett.*, 25, 1999–2002.

Thurber, C. (1983) Earthquake locations and three-dimensional crustal structure in the Coyote Lake area, central California. *J. Geophys. Res.*, 88, 8226–8236.

Thurber, C., and K. Aki (1987) Three-dimensional seismic imaging. *Ann. Rev. Earth Planet. Sci.*, 15, 115–139.

Tilmann, F., H. Benz, K. Priestley, and P. Okubo (2001) P-wave velocity structure of the uppermost mantle beneath Hawaii from travel time tomography. *Geophys. J. Int.*, 146, 594–606.

Tryggvason, K., E. Husebye, and R. Stefansson (1983) Seismic image of the hypothesized Icelandic hot spot. *Tectonophysics*, 100, 97–118.

Tsuchiya, T., J. Tsuchiya, K. Umemoto, and R. Wentzcovitch (2004) Phase transition in MgSiO3 perovskite in the earth's lower mantle. *Earth Planet. Sci. Lett.*, 224, 241–248.

Tsumura, N., S. Matsumoto, S. Horiuchi, and A. Hasegawa (2000) Three-dimensional attenuation structure beneath the northeastern Japan arc estimated from spectra of small earthquakes. *Tectonophysics*, 319, 241–260.

Turcotte, D., and E. Oxburgh (1973) Mid-plate tectonics. *Nature*, 244, 337–339.

Turcotte, D., and G. Schubert (1982) Geodynamics, John Wiley and Sons Press, New York, 450pp.

Umino, N., A. Hasegawa, and T. Matsuzawa (1995) sP depth phase at small epicentral distances and estimated subducting plate boundary. *Geophys. J. Int.*, 120, 356–366.

Ukawa, M., and K. Obara (1993) Low frequency earthquakes around Moho beneath the volcanic front in the Kanto district, central Japan. *Bull. Volcanol. Soc. Jpn.*, 38, 187–197.

van der Hilst, R., and M. de Hoop (2005) Banana-doughnut kernels and mantle tomography. *Geophys. J. Int.*, 163, 956–961.

van der Hilst, R., S. Widiyantoro, and E. Engdahl (1997) Evidence for deep mantle circulation from global tomography. *Nature*, 386, 578–584.

Van der Voo, R., W. Spakman, and H. Bijwaard (1999a) Mesozoic subducted slabs under Siberia. *Nature*, 397, 246–249.

Van der Voo, R., W. Spakman, and H. Bijwaard (1999b) Tethyan subducted slabs under India. *Earth Planet. Sci. Lett.*, 171, 7–20.

Vasco, D., L. Johnson, and R. Pulliam (1995) Lateral variations in mantle velocity structure and discontinuities determined from P, PP, S, SS, and SS-SdS travel time residuals. *J. Geophys. Res.*, 100, 24037–24059.

Vinnik, L., L. Breger, and B. Romanowicz (1998) Anisotropic structures at the base of the mantle. *Nature*, 393, 564–567.

Vogt, P. (1981) On the applicability of thermal conduction models to mid-plate volcanism, comments on a paper by Gass et al. *J. Geophys. Res.*, 86, 950–960.

Wang, Z., and D. Zhao (2005) Seismic imaging of the entire arc of Tohoku and Hokkaido in Japan using P-wave, S-wave and sP depth-phase data. *Phys. Earth Planet. Inter.*, 152, 144–162.

Weinstein, S., and P. Olson (1989) The proximity of hotspots to convergent and divergent plate boundaries. *Geophys. Res. Lett.*, 16, 433–436.

Williams, Q., and E. Garnero (1996) Seismic evidence for partial melt at the base of Earth's mantle. *Science*, 273, 1528–1530.

Wilson, J. (1963) A possible origin of the Hawaiian islands. *Can. J. Phys.*, 41, 863–870.

Wilson, J. (1973) Mantle plumes and plate motions. *Tectonophysics*, 19, 149–164.

Wolfe, C., I. Bjarnason, J. VanDecar, and S. Soloman (1997) Seismic structure of the Iceland mantle plume. *Nature*, 385, 245–247.

Wolfe, C., S. Solomon, P. Silver, J. VanDecar, and R. Russo (2002) Inversion of body-wave delay times for mantle structure beneath the Hawaiian islands: Results from the PELENET experiment. *Earth Planet. Sci. Lett.*, 198, 129–145.

Woodhouse, J., and A. Dziewonski (1984) Mapping the upper mantle: Three-dimensional modeling of earth structure by inversion of seismic waveforms. *J. Geophys. Res.*, 89, 5953–5986.

Woods, M., and E. Okal (1996) Rayleigh-wave dispersion along the Hawaiian swell: A test of lithospheric thinning by thermal rejuvenation at a hotspot. *Geophys. J. Int.*, 125, 325–339.

Woodward, R., and G. Master (1991) Lower mantle structure from ScS-S differential travel times. *Nature*, 352, 231–233.

Wysession, M., T. Lay, and J. Revenaugh (1998) The D″ discontinuity and its implications. In Gurnis, M., B. Buffett, K. Knittle, M. Wysession (eds.) The Core-Mantle Boundary, AGU, pp. 273–297.

Yuan, H., and K. Dueker (2005) Teleseismic P-wave tomogram of the yellowstone plume. *Geophys. Res. Lett.*, 32(7), L07304.

Yuen, D., O. Cadek, A. Chopelas, and C. Matyska (1993) Geophysical inferences of thermal-chemical structures in the lower mantle. *Geophys. Res. Lett.*, 20, 899–902.

Zhang, Y., and T. Tanimoto (1993) High-resolution global upper mantle structure and plate tectonics. *J. Geophys. Res.*, 98, 9793–9823.

Zhao, D. (2001a) New advances of seismic tomography and its applications to subduction zones and earthquake fault zones. *The Island Arc*, 10, 68–84.

Zhao, D. (2001b) Seismological structure of subduction zones and its implications for arc magmatism and dynamics. *Phys. Earth Planet. Inter.*, 127, 197–214.

Zhao, D. (2001c) Seismic structure and origin of hotspots and mantle plumes. *Earth Planet. Sci. Lett.*, 192, 251–265.

Zhao, D. (2004) Global tomographic images of mantle plumes and subducting slabs: Insight into deep Earth dynamics. *Phys. Earth Planet. Inter.*, 146, 3–34.

Zhao, D., A. Hasegawa, and S. Horiuchi (1992) Tomographic imaging of P and S wave velocity structure beneath northeastern Japan. *J. Geophys. Res.*, 97, 19909–19928.

Zhao, D., A. Hasegawa, and H. Kanamori (1994) Deep structure of Japan subduction zone as derived from local, regional and teleseismic events. *J. Geophys. Res.*, 99, 22313–22329.

Zhao, D., D. Christensen, and H. Pulpan (1995) Tomographic imaging of the Alaska subduction zone. *J. Geophys. Res.*, 100, 6487–6504.

Zhao, D., Y. Xu, D. Wiens, L. Dorman, J. Hildebrand, and S. Webb (1997) Depth extent of the Lau back-arc spreading center and its relation to subduction processes. *Science*, 278, 254–257.

Zhao, D., K. Asamori, and H. Iwamori (2000) Seismic structure and magmatism of the young Kyushu subduction zone. *Geophys. Res. Lett.*, 27, 2057–2060.

Zhao, D., O.P. Mishra, and R. Sanda (2002) Influence of fluids and magma on earthquakes: Seismological evidence. *Phys. Earth Planet. Inter.*, 132, 249–267.

Zhao, D., J. Lei, and R. Tang (2004) Origin of the Changbai intraplate volcanism in Northeast China: Evidence from seismic tomography. *Chinese Sci. Bull.*, 49, 1401–1408.

Zhao, D., S. Todo, and J. Lei (2005) Local earthquake reflection tomography of the Landers aftershock area. *Earth Planet. Sci. Lett.*, 235, 623–631.

Zhao, D., J. Lei, T. Inoue, A. Yamada, and S. Gao (2006) Deep structure and origin of the Baikal rift zone. *Earth Planet. Sci. Lett.*, 243, 681–691.

Zhou, H. (1996) A high-resolution P wave model for the top 1200 km of the mantle. *J. Geophys. Res.*, 101, 27791–27810.